Theory of Reverberation in Rectangular Rooms with Surface Scattering

Tetsuya Sakuma
Graduate School of Frontier Sciences, University of Tokyo, Kashiwa, Japan.

Summary
Firstly a theory of reverberation in rectangular rooms is formulated on the condition that only specular reflections occur from image sources. It is based on the idea that image sources are divided into the axial, tangential and oblique groups, which chiefly contribute to the corresponding normal mode groups in wave acoustics. As a result, the reverberation formula for rectangular rooms consists of seven kinds of exponential decay. Secondly, surface scattering is considered by introducing scattering coefficients to the above formula. The specular reflection field is simply formulated by substituting specular absorption coefficients, while the diffuse reflection field, in which energy is transformed from the specular reflection field at each reflection, is formulated with the decay in three-dimensional diffuse field.

PACS no. 43.55.Br, 43.20.Fn

1. Introduction

A variety of reverberation theories in rooms exist, originated from Sabine's equation [1] on the assumption of diffuse field, modified by Eyring-Norris [2, 3], Millington-Sette [4, 5], Kuttruff [6, 7], and for rectangular rooms, proposed by Fitzroy [8], Pujolle [9], Hirata [10], Arau-Puchades [11], Nilsson [12], Neubauer [13] etc.. As an interesting approach to non-diffuse field, Hirata derived a reverberation theory by the image source method, decomposing 1D, 2D and 3D fields. However, the theoretical development has a misunderstanding on field decomposition, and furthermore, room for reconsideration on average absorption coefficients. In this paper, firstly, a reverberation theory for specular reflection field in rectangular rooms is formulated by modifying Hirata's theory. Secondly, considering surface scattering on the walls with scattering coefficients, an integrated reverberation theory for non-diffuse field is newly developed.

2. Reverberation of specular reflection field in rectangular rooms

2.1. Specular field of image sources

Consider the arrangement of image sources for a point source in a rectangular room (Figure 1), and estimate the number of sources in a very small

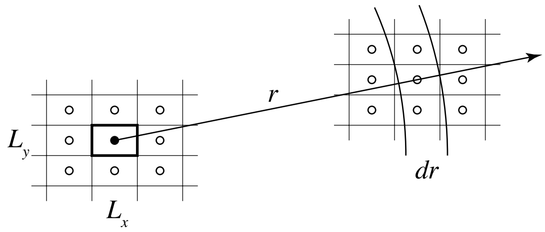

Figure 1. Image sources of a rectangular room.

path at equal distance from a receiving point, distance attenuation and wall absorption. If the source is stopped at $t=0$ in steady state, the energy density of specular reflection field in the room is expressed by

$$E_{\mathrm{ob}}^{\mathrm{S}}(t)=\int_{ct}^{\infty}\frac{W}{4\pi cr^2}\left(1-\alpha_{\mathrm{ob}}\right)^{\frac{r}{l_{\mathrm{ob}}}}\frac{4\pi r^2 dr}{V}=\frac{4W}{cA_{\mathrm{ob}}}e^{-\frac{\alpha_{\mathrm{Eob}}}{l_{\mathrm{ob}}}ct}$$

$(t\geq 0)$ (1)

where the 3D mean free path $l_{\mathrm{ob}}\approx l_{\mathrm{r}}=4V/S$, the room volume V, the total surface area S, $A_{\mathrm{ob}}=S\alpha_{\mathrm{Eob}}$, $\alpha_{\mathrm{Eob}}=-\ln\left(1-\alpha_{\mathrm{ob}}\right)$,

$$\alpha_{\mathrm{ob}}=2\left(L_yL_z\tilde{\alpha}_x^{\mathrm{r}}+L_zL_x\tilde{\alpha}_y^{\mathrm{r}}+L_xL_y\tilde{\alpha}_z^{\mathrm{r}}\right)/S \quad (2)$$

$$\tilde{\alpha}_{x(y,z)}^{\mathrm{r}}=1-\sqrt{\left(1-\alpha_{x(y,z)}^{\mathrm{r}+}\right)\left(1-\alpha_{x(y,z)}^{\mathrm{r}-}\right)} \quad (3)$$

$\alpha_{x(y,z)}^{\mathrm{r}\pm}$ are the random-incidence absorption coefficients of two parallel walls, $\tilde{\alpha}_{x(y,z)}^{\mathrm{r}}$ is the geometrical mean for alternate reflections between the walls, and α_{ob} is assumed the area-weighted mean for the three directions. The above equation roughly corresponds to the specular field of oblique sources. In the following, other specular

(c) European Acoustics Association

fields are considered by dividing image sources into axial, tangential and oblique groups, which chiefly contribute to 1D, 2D and 3D specular fields, respectively.

2.2. Specular fields of axial sources

Consider the image sources near the x-axis in the angular ranges within $\pm\theta_{\mathrm{ax}y}$ and within $\pm\theta_{\mathrm{ax}z}$ to the positive and negative x-directions (Figure 2), which lead to normal incidence for x-directional walls (yz-plane), and glazing incidence for y-/z-directional walls. In the above ranges, if the path differences from a far image source in y-/z-directions are within 1/4 wavelength (π/2 in phase), the source chiefly contribute to the corresponding axial modes in the wave theory. The path differences are $\Delta_{xy(z)} \approx L_{y(z)} \sin\theta_{\mathrm{ax}y(z)} \approx L_{y(z)}\theta_{\mathrm{ax}y(z)}$, which giving the critical angles

$$\theta_{\mathrm{ax}y(z)} = \pi c / 2\omega L_{y(z)} \tag{4}$$

At the angles, the frequency of reflections for x-directional walls $n_{\mathrm{ax}} \approx c/L_x$, while those for y-/z-directional walls $n_{\mathrm{ax}y(z)} \approx c\theta_{\mathrm{ax}y(z)}/L_{y(z)}$. In the angular ranges, the average frequencies $\bar{n}_{\mathrm{ax}} \approx n_{\mathrm{ax}}$, while $\bar{n}_{\mathrm{a}y(z)} \approx n_{\mathrm{a}y(z)}/2$. Similarly to Eq. (1), the energy density of specular field from x-axial sources is given by

$$E_{\mathrm{ax}}^{\mathrm{S}}(t) = \frac{4W}{c}\int_{ct}^{\infty}\left(1-\tilde{\alpha}_x^{\mathrm{n}}\right)^{\frac{r}{L_x}}\left(1-\tilde{\alpha}_y^{\mathrm{g}}\right)^{\frac{\theta_{\mathrm{ax}y}r}{2L_y}}\left(1-\tilde{\alpha}_z^{\mathrm{g}}\right)^{\frac{\theta_{\mathrm{ax}z}r}{2L_z}} \cdot \frac{2\left(2\theta_{\mathrm{ax}y}\right)\left(2\theta_{\mathrm{ax}z}\right)dr}{4\pi V}$$

$$= \frac{4W}{c}\frac{\pi c^2 L_x}{2\omega^2 V^2}\int_{ct}^{\infty}\left(1-\alpha_{\mathrm{ax}}\right)^{\frac{r}{l_x}}dr = \frac{4W}{c}\frac{2\pi c^2 L_x}{\omega^2 V\hat{A}_{\mathrm{ax}}}e^{-\frac{\alpha_{\mathrm{Eax}}}{l_x}ct} \tag{5}$$

where the 1D mean free path $l_x = L_x$,

$\hat{A}_{\mathrm{ax}} = 2A_{\mathrm{ax}}$, $A_{\mathrm{ax}} = 2L_yL_z\alpha_{\mathrm{Eax}}$, $\alpha_{\mathrm{Eax}} = -\ln\left(1-\alpha_{\mathrm{ax}}\right)$,

$$\alpha_{\mathrm{ax}} = 1-\left(1-\tilde{\alpha}_x^{\mathrm{n}}\right)\left(1-\tilde{\alpha}_y^{\mathrm{g}}\right)^{\varepsilon_{\mathrm{ax}y}}\left(1-\tilde{\alpha}_z^{\mathrm{g}}\right)^{\varepsilon_{\mathrm{ax}z}} \tag{6}$$

$$\varepsilon_{\mathrm{ax}y(z)} = \frac{\bar{n}_{\mathrm{ax}y(z)}}{\bar{n}_{\mathrm{ax}}} \approx \frac{\pi c L_x}{4\omega L_{y(z)}^2} \tag{7}$$

$\tilde{\alpha}_x^{\mathrm{n}}$ is the normal-incidence absorption coefficient of x-directional walls, and $\tilde{\alpha}_{y(z)}^{\mathrm{g}}$ are the glazing-incidence values of y-/z-directional walls, where considering the geometrical mean for parallel walls according to Eq. (3). The total average value for the 1D field, α_{ax}, is given by taking into account the frequency of reflections in every direction, with $\varepsilon_{\mathrm{ax}y(z)}$ the average frequency ratio of y-/z-directional to x-directional walls. Note that in Eq. (5) the contribution of axial sources to 1D field is four times that of oblique sources to 3D field, which corresponds to the ratio of normalization factors in the mode theory.

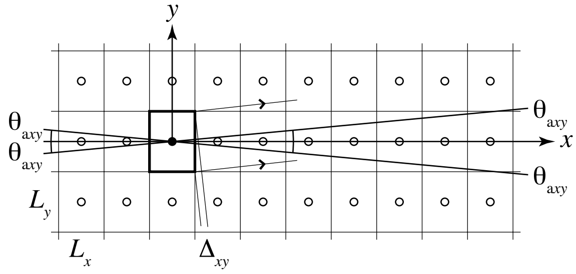

Figure 2. Axial image sources for x-axis in xy-plane.

2.3. Specular fields of tangential sources

In a similar way to axial sources, consider the image sources near the xy-plane in the angular range within $\pm\theta_{\mathrm{t}z}$ to the xy-plane, which lead to random incidence for x-/y-directional walls, and glazing incidence for z-directional walls (xy-plane). The critical angle is given by

$$\theta_{\mathrm{t}z} = \pi c / 2\omega L_z \tag{8}$$

In the anglular range, the average frequency of reflections for x- and y-directional walls is $\bar{n}_{\mathrm{t}xy} \approx n_{\mathrm{t}xy} \approx c/l_{xy}$, where the 2D mean free path $l_{xy} = \pi L_x L_y / 2\left(L_x + L_y\right)$, and that for z-directional walls $\bar{n}_{\mathrm{t}z} \approx n_{\mathrm{t}z}/2 \approx c\theta_{\mathrm{t}z}/2L_z$. Similarly to Eq. (5), the energy density of specular field from xy-tangential sources is given by

$$E_{\mathrm{t}xy}^{\mathrm{S}}(t) = \frac{2W}{c}\int_{ct}^{\infty}\left(1-\tilde{\alpha}_{xy}^{\mathrm{r}}\right)^{\frac{r}{l_{xy}}}\left(1-\tilde{\alpha}_z^{\mathrm{g}}\right)^{\frac{\theta_{\mathrm{t}z}r}{2L_z}}\frac{2\pi\left(2\theta_{\mathrm{t}z}\right)dr}{4\pi V}$$

$$= \frac{2W}{c}\frac{\pi c L_x L_y}{2\omega V^2}\int_{ct}^{\infty}\left(1-\alpha_{\mathrm{t}xy}\right)^{\frac{r}{l_{xy}}}dr = \frac{4W}{c}\frac{\pi c L_x L_y}{\omega V\hat{A}_{\mathrm{t}xy}}e^{-\frac{\alpha_{\mathrm{Et}xy}}{l_{xy}}ct} \tag{9}$$

where $\hat{A}_{\mathrm{t}xy} = \left(4/\pi\right)A_{\mathrm{t}xy}$, $A_{\mathrm{t}xy} = 2\left(L_x + L_y\right)L_z\alpha_{\mathrm{Et}xy}$,

$\alpha_{\mathrm{Et}xy} = -\ln\left(1-\alpha_{\mathrm{t}xy}\right)$,

$$\alpha_{\mathrm{t}xy} = 1-\left(1-\tilde{\alpha}_{xy}^{\mathrm{r}}\right)\left(1-\tilde{\alpha}_z^{\mathrm{g}}\right)^{\varepsilon_{\mathrm{t}z}} \tag{10}$$

$$\tilde{\alpha}_{xy}^{\mathrm{r}} = \left(L_y\tilde{\alpha}_x^{\mathrm{r}} + L_x\tilde{\alpha}_y^{\mathrm{r}}\right)/\left(L_x + L_y\right) \tag{11}$$

$$\varepsilon_{\mathrm{t}z} = \frac{\bar{n}_{\mathrm{t}z}}{\bar{n}_{\mathrm{t}xy}} \approx \frac{\pi^2 c L_x L_y}{8\omega\left(L_x + L_y\right)L_z^2} \tag{12}$$

$\tilde{\alpha}_{xy}^{\mathrm{r}}$ is the area-weighted mean random-incidence value for the two directions, and $\alpha_{\mathrm{t}xy}$ is the total average value for the 2D field, with $\varepsilon_{\mathrm{t}z}$ the ratio of average reflection frequencies of z-directional to x- and y-directional walls. Note that in Eq. (9) the contribution of tangential sources to 2D field is twice that of oblique sources to 3D field.

2.4. Reverberation of total specular field

Equation (1) includes the contributions of axial and tangential sources, and Eq. (9) includes that of axial sources. Excluding these contributions, and

 (c) European Acoustics Association, ISBN: 978-84-694-1520-7, ISSN: 221-3767

summing up Eqs. (1), (5) and (9), the total energy density of specular field in the room is given by

$$E^{\mathrm{S}}(t)=\frac{4W}{c}\left[\frac{\gamma_{\mathrm{ob}}}{A_{\mathrm{ob}}}e^{-\frac{\alpha_{\mathrm{Eob}}}{l_{\mathrm{ob}}}ct}+\sum_{xy}\frac{\gamma_{\mathrm{t}xy}\pi cL_xL_y}{\omega V\hat{A}_{\mathrm{t}xy}}e^{-\frac{\alpha_{\mathrm{Et}xy}}{l_{xy}}ct}+\sum_{x}\frac{2\pi c^2L_x}{\omega^2V\hat{A}_{\mathrm{a}x}}e^{-\frac{\alpha_{\mathrm{Ea}x}}{l_x}ct}\right] \tag{13}$$

where $\gamma_{\mathrm{ob}}=1-\pi cS/4\omega V+\pi c^2L/8\omega^2V$,
$\gamma_{\mathrm{t}xy}=1-c\left(L_x+L_y\right)/\omega L_xL_y$,
$L=4\left(L_x+L_y+L_z\right)$,
thus the reverberation of the total specular field is composed of seven kinds of exponential decay, arising from one oblique, three tangential and three axial source groups. Each decay rate is given by

$$D^{\mathrm{S}}_{\mathrm{ob(t}xy,\mathrm{a}x)}=10\lg e\cdot c\,\alpha_{\mathrm{Eob(t}xy,\mathrm{a}x)}/l_{\mathrm{ob}(xy,x)} \tag{14}$$

2.5. Correspondece to wave theory

Equation (13) entirely corresponds to the equation derived from the mode theory [14]. The critical angles for axial and tangential image sources can be interpreted in view of normal mode distribution in wavenumber space (Figure 3). Supposing the ranges dominated by axial modes to be within the middle to the adjacent oblique modes, the critical angles are determined depending on wavenumber as follows

$$\pi/2L_{y(z)}=k\sin\theta_{\mathrm{a}xy(z)}\approx k\theta_{\mathrm{a}xy(z)} \tag{15}$$

which is consistent with Eq. (4). Thus it can be stated that the angular ranges for axial/tangential image sources approximately correspond to the axial/tangential modes in wavenumber space. Note that Hirata [10] determined different angular ranges from the above in an ambiguous discussion, and also used the arithmetic means wighted with the reflection frequency of every direction as the total average absorption coefficients, which finally leading to different decay rates.

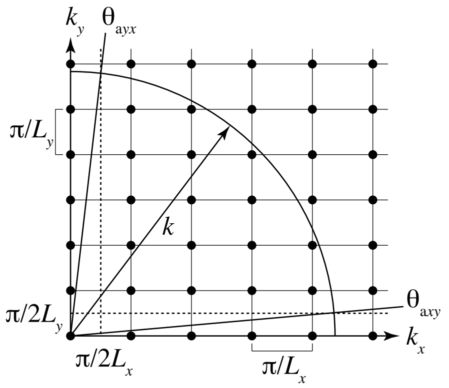

Figure 3. Axial modes in *xy*-plane in *k*-space.

3. Reverberation in rectangular rooms with surface scattering

3.1. Specular field with surface scattering

The sound energy propagating from image sources can be divided into specular and diffuse reflection components by introducing scattering coefficients of wall surfaces [15]. Considering the specular field as not scattered throughout every path from a source to a receiving point (Figure 4), the energy density is given by replacing all values related to absorption coefficient with those related to specular absorption coefficient $\beta=\alpha+(1-\alpha)s$, where s is the scattering coefficient. Accordingly, Eq. (13) is modified by substituting all kinds of $\tilde{\beta}$, β_{E}, B and $\hat{B}$ for $\tilde{\alpha}$, α_{E}, A, and $\hat{A}$.

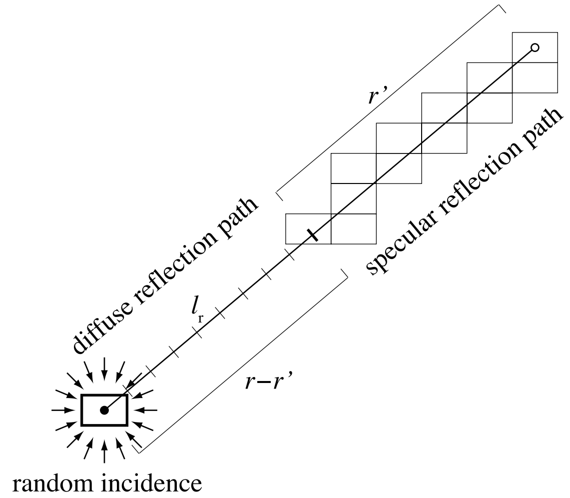

Figure 4. Transition from specular to diffuse reflections.

3.2. Diffuse field with surface scattering

It is considered that a part of specular energy is transformed into diffuse energy at every reflection, and after the transition, the energy is decayed by perfectly diffuse reflections in the 3D diffuse field. Estimating the energy scattered at an arbitrary distance r' from a source and decayed before and after the transition, and integrating it with respect to r' throughout every path, the energy density of diffuse field is given by

$$\begin{aligned}E^{\mathrm{D}}_{\mathrm{ob}}(t)&=\frac{W}{c}\int_{ct}^{\infty}\int_{0}^{r}\left(1-\beta_{\mathrm{ob}}\right)^{\frac{r'}{l_{\mathrm{ob}}}}\left(1-\alpha_{\mathrm{r}}\right)^{\frac{r-r'}{l_{\mathrm{r}}}}\frac{s_{\mathrm{Eob}}dr'}{l_{\mathrm{ob}}}\frac{dr}{V}\\&=\frac{W}{c}\mu_{\mathrm{ob}}\int_{ct}^{\infty}\left(\left(1-\alpha_{\mathrm{r}}\right)^{\frac{r}{l_{\mathrm{r}}}}-\left(1-\beta_{\mathrm{ob}}\right)^{\frac{r}{l_{\mathrm{ob}}}}\right)\frac{dr}{V}\\&=\frac{4W}{c}\mu_{\mathrm{ob}}\left(\frac{1}{A_{\mathrm{r}}}e^{-\frac{\alpha_{\mathrm{Er}}}{l_{\mathrm{r}}}ct}-\frac{1}{B_{\mathrm{ob}}}e^{-\frac{\beta_{\mathrm{Eob}}}{l_{\mathrm{ob}}}ct}\right)\end{aligned} \tag{16}$$

where $\mu_{\mathrm{ob}}=\dfrac{s_{\mathrm{Eob}}/l_{\mathrm{ob}}}{\beta_{\mathrm{Eob}}/l_{\mathrm{ob}}-\alpha_{\mathrm{Er}}/l_{\mathrm{r}}}$,

(c) European Acoustics Association, ISBN: 978-84-694-1520-7, ISSN: 221-3767

$A_\mathrm{r} = S\alpha_\mathrm{Er}$, $\alpha_\mathrm{Er} = -\ln(1-\alpha_\mathrm{r})$, $s_\mathrm{Eob} = -\ln(1-s_\mathrm{ob})$,

$\beta_\mathrm{Eob} = -\ln(1-\beta_\mathrm{ob}) = \alpha_\mathrm{Eob} + s_\mathrm{Eob}$,

$$s_\mathrm{ob} = \frac{L_y L_z \tilde{r}_x^\mathrm{r} \tilde{s}_x^\mathrm{r} + L_z L_x \tilde{r}_y^\mathrm{r} \tilde{s}_y^\mathrm{r} + L_x L_y \tilde{r}_z^\mathrm{r} \tilde{s}_z^\mathrm{r}}{L_y L_z \tilde{r}_x^\mathrm{r} + L_z L_x \tilde{r}_y^\mathrm{r} + L_x L_y \tilde{r}_z^\mathrm{r}} \tag{17}$$

$\tilde{r}_{x(y,z)}^\mathrm{r} = 1 - \tilde{\alpha}_{x(y,z)}^\mathrm{r}$,

α_r is the area-weighted mean of random-incidence absorption coefficients, $\tilde{s}_{x(y,z)}^\mathrm{r}$ is the geometrical mean of random-incidence scattering coefficients of two parallel walls, and s_ob is assumed the arithmetic mean weighted with the area and the reflection coefficient of every direction. In Eq. (16), the rate of scattered energy in a very small path is given by

$$\lim_{dr' \to 0} 1 - (1-s_\mathrm{ob})^{\frac{dr'}{l_\mathrm{ob}}} = \lim_{dr' \to 0} 1 - e^{-\frac{s_\mathrm{Eob} dr'}{l_\mathrm{ob}}} \to \frac{s_\mathrm{Eob} dr'}{l_\mathrm{ob}} \tag{18}$$

Note that for oblique sources the relations $l_\mathrm{ob} \approx l_\mathrm{r}$ and $\alpha_\mathrm{ob} \geq \alpha_\mathrm{r}$ result in $0 \leq \mu_\mathrm{ob} \leq 1$ and $B_\mathrm{ob} \geq A_\mathrm{r}$.

3.3. Diffuse fields of axial sources

Similarly to the above section, the energy density of diffuse field from *x*-axial sources is given by

$$\begin{aligned} E_\mathrm{ax}^\mathrm{D}(t) &= \frac{W}{c} \int_{ct}^{\infty} \int_0^r \left(1-\tilde{\beta}_x^\mathrm{n}\right)^{\frac{r'}{L_x}} \left(1-\tilde{\beta}_y^\mathrm{g}\right)^{\frac{\theta_{axy} r'}{2L_y}} \left(1-\tilde{\beta}_z^\mathrm{g}\right)^{\frac{\theta_{axz} r'}{2L_z}} \\ &\quad \cdot (1-\alpha_\mathrm{r})^{\frac{r-r'}{l_\mathrm{r}}} \frac{s_\mathrm{Eax} dr'}{l_x} \frac{2(2\theta_{xy})(2\theta_{xz}) dr}{4\pi V} \\ &= \frac{W}{c} \frac{\pi c^2 L_x}{2\omega^2 V} \int_{ct}^{\infty} \int_0^r (1-\beta_\mathrm{ax})^{\frac{r'}{l_x}} (1-\alpha_\mathrm{r})^{\frac{r-r'}{l_\mathrm{r}}} \frac{s_\mathrm{Eax} dr'}{l_x} \frac{dr}{V} \\ &= \frac{W}{c} \frac{2\pi c^2 L_x}{\omega^2 V} \mu_\mathrm{ax} \left(\frac{1}{A_\mathrm{r}} e^{-\frac{\alpha_\mathrm{Er}}{l_\mathrm{r}} ct} - \frac{1}{\hat{B}_\mathrm{ax}} e^{-\frac{\beta_\mathrm{Eax}}{l_x} ct} \right) \end{aligned} \tag{19}$$

where $\mu_\mathrm{ax} = \dfrac{s_\mathrm{Eax}/l_\mathrm{x}}{\beta_\mathrm{Eax}/l_\mathrm{x} - \alpha_\mathrm{Er}/l_\mathrm{r}}$, $s_\mathrm{Eax} = -\ln(1-s_\mathrm{ax})$,

s_ax is the total average scattering coefficient given similarly to Eq. (6), with $\tilde{s}_x^\mathrm{n}$ the normal-incidence value of *x*-directional walls and $\tilde{s}_{y(z)}^\mathrm{g}$ the glazing-incidence values of *y*-/*z*-directional walls, as the geometrical mean for parallel walls. In contrast to Eq. (5), the above equation do not involve the ratio of normalization factors for axial modes. If $\beta_\mathrm{Eax}/l_\mathrm{x} > \alpha_\mathrm{Er}/l_\mathrm{r}$, $\mu_\mathrm{ax} \geq 0$ and $\hat{B}_\mathrm{ax} > A_\mathrm{r}$, otherwise changing the signs of inequality. In a singular case that $\beta_\mathrm{Eax}/l_\mathrm{x} = \alpha_\mathrm{Er}/l_\mathrm{r}$, Eq. (19) can be transformed into

$$E_\mathrm{ax}^\mathrm{D}(t) = \frac{W}{c} \frac{2\pi c^2 L_x}{\omega^2 V} \frac{s_\mathrm{Eax}}{\beta_\mathrm{Eax}} \left(1 + \frac{\alpha_\mathrm{Er}}{l_\mathrm{r}} ct\right) \frac{1}{A_\mathrm{r}} e^{-\frac{\alpha_\mathrm{Er}}{l_\mathrm{r}} ct} \tag{20}$$

3.4. Diffuse fields of tangential fields

Similarly to axial sources, the energy density of diffuse field from *xy*-tangential sources is given by

$$\begin{aligned} E_\mathrm{txy}^\mathrm{D}(t) &= \frac{W}{c} \int_{ct}^{\infty} \int_0^r \left(1-\tilde{\beta}_{xy}^\mathrm{r}\right)^{\frac{r'}{l_{xy}}} \left(1-\tilde{\beta}_z^\mathrm{g}\right)^{\frac{\theta_{tz} r'}{2L_z}} \\ &\quad \cdot (1-\alpha_\mathrm{r})^{\frac{r-r'}{l_\mathrm{r}}} \frac{s_\mathrm{Etxy} dr'}{l_\mathrm{txy}} \frac{2\pi(2\theta_z) dr}{4\pi V} \\ &= \frac{W}{c} \frac{\pi c L_x L_y}{2\omega V} \int_{ct}^{\infty} \int_0^r (1-\beta_\mathrm{txy})^{\frac{r'}{l_{xy}}} (1-\alpha_\mathrm{r})^{\frac{r-r'}{l_\mathrm{r}}} \frac{s_\mathrm{Etxy} dr'}{l_{xy}} \frac{dr}{V} \\ &= \frac{W}{c} \frac{2\pi c L_x L_y}{\omega V} \mu_\mathrm{txy} \left(\frac{1}{A_\mathrm{r}} e^{-\frac{\alpha_\mathrm{Er}}{l_\mathrm{r}} ct} - \frac{1}{\hat{B}_\mathrm{txy}} e^{-\frac{\beta_\mathrm{Etxy}}{l_{xy}} ct} \right) \end{aligned} \tag{21}$$

where $\mu_\mathrm{txy} = \dfrac{s_\mathrm{Etxy}/l_\mathrm{xy}}{\beta_\mathrm{Etxy}/l_\mathrm{xy} - \alpha_\mathrm{Er}/l_\mathrm{r}}$, $s_\mathrm{Etxy} = -\ln(1-s_\mathrm{txy})$,

s_txy is the total average scattering coefficient given similarly to Eqs. (10) and (11), with modifying the latter as

$$\tilde{s}_{xy}^\mathrm{r} = \left(L_y \tilde{r}_x^\mathrm{r} \tilde{s}_x^\mathrm{r} + L_x \tilde{r}_y^\mathrm{r} \tilde{s}_y^\mathrm{r}\right) / \left(L_x \tilde{r}_x^\mathrm{r} + L_y \tilde{r}_y^\mathrm{r}\right) \tag{22}$$

where assuming the arithmetic mean weighted with area and reflection coefficient. Again, if $\beta_\mathrm{Etxy}/l_\mathrm{xy} > \alpha_\mathrm{Er}/l_\mathrm{r}$, $\mu_\mathrm{txy} \geq 0$ and $\hat{B}_\mathrm{txy} > A_\mathrm{r}$, otherwise changing the signs of inequality, and in a singular case that $\beta_\mathrm{Etxy}/l_\mathrm{xy} = \alpha_\mathrm{Er}/l_\mathrm{r}$, Eq. (21) can be transformed into

$$E_\mathrm{ax}^\mathrm{D}(t) = \frac{W}{c} \frac{2\pi c L_x L_y}{\omega V} \frac{s_\mathrm{Etxy}}{\beta_\mathrm{Etxy}} \left(1 + \frac{\alpha_\mathrm{Er}}{l_\mathrm{r}} ct\right) \frac{1}{A_\mathrm{r}} e^{-\frac{\alpha_\mathrm{Er}}{l_\mathrm{r}} ct} \tag{23}$$

3.5. Reverberation of total diffuse field

Similarly to specular field, summing up Eqs. (16), (19) and (21) with excluding the duplicate contributions, the total energy density of diffuse field in the room is given by

$$\begin{aligned} E^\mathrm{D}(t) = \frac{4W}{c} \Bigg[& \gamma_\mathrm{ob} \mu_\mathrm{ob} \left(\frac{1}{A_\mathrm{r}} e^{-\frac{\alpha_\mathrm{Er}}{l_\mathrm{r}} ct} - \frac{1}{B_\mathrm{ob}} e^{-\frac{\beta_\mathrm{Eob}}{l_\mathrm{ob}} ct} \right) \\ & + \sum_{xy} \frac{\gamma_\mathrm{txy} \pi c L_x L_y}{2\omega V} \mu_\mathrm{txy} \left(\frac{1}{A_\mathrm{r}} e^{-\frac{\alpha_\mathrm{Er}}{l_\mathrm{r}} ct} - \frac{1}{\hat{B}_\mathrm{txy}} e^{-\frac{\beta_\mathrm{Etxy}}{l_{xy}} ct} \right) \\ & + \sum_{x} \frac{\pi c^2 L_x}{2\omega^2 V} \mu_\mathrm{ax} \left(\frac{1}{A_\mathrm{r}} e^{-\frac{\alpha_\mathrm{Er}}{l_\mathrm{r}} ct} - \frac{1}{\hat{B}_\mathrm{ax}} e^{-\frac{\beta_\mathrm{Eax}}{l_x} ct} \right) \Bigg] \end{aligned} \tag{24}$$

From the above, the steady state energy density at $t = 0$ is expressed by

$$\begin{aligned} E^\mathrm{D}(0) = \frac{4W}{cA_\mathrm{r}} \Bigg(& \gamma_\mathrm{ob} \frac{s_\mathrm{Eob}}{\beta_\mathrm{Eob}} + \sum_{xy} \frac{\gamma_\mathrm{txy} \pi c L_x L_y}{2\omega V} \frac{s_\mathrm{Etxy}}{\beta_\mathrm{Etxy}} \\ & + \sum_{x} \frac{\pi c^2 L_x}{2\omega^2 V} \frac{s_\mathrm{Eax}}{\beta_\mathrm{Eax}} \Bigg) \end{aligned} \tag{25}$$

The reverberation of the total diffuse field is also apparently composed of seven kinds of decay, but not pure exponential decay. With the decay rate of the 3D diffuse field $D_\mathrm{r}^\mathrm{D} = 10 \lg e \cdot c\alpha_\mathrm{Er}/l_\mathrm{r}$, the rates for source groups are given by

(c) European Acoustics Association, ISBN: 978-84-694-1520-7, ISSN: 221-3767

$$D_{\mathrm{ob}}^{\mathrm{D}}(t) = D_{\mathrm{r}}^{\mathrm{D}} \frac{1 - e^{-\left(\frac{\beta_{\mathrm{Eob}}}{l_{\mathrm{ob}}} - \frac{\alpha_{\mathrm{Er}}}{l_{\mathrm{r}}}\right)ct}}{1 - \left(A_{\mathrm{r}}/B_{\mathrm{ob}}\right) e^{-\left(\frac{\beta_{\mathrm{Eob}}}{l_{\mathrm{ob}}} - \frac{\alpha_{\mathrm{Er}}}{l_{\mathrm{r}}}\right)ct}} \tag{26}$$

and $D_{\mathrm{t}xy(\mathrm{a}x)}^{\mathrm{D}}(t)$ with substituting $\hat{B}_{\mathrm{t}xy(\mathrm{a}x)}$, $\beta_{\mathrm{Et}xy(\mathrm{a}x)}$ and $l_{xy(x)}$ for B_{ob}, β_{Eob} and l_{ob}. Just after stopping the source ($t \to 0$), $D_{\mathrm{ob(t}xy,\mathrm{a}x)}^{\mathrm{D}}(t) \to 0$ for all seven components. On the other hand, after a long time ($t \to \infty$), $D_{\mathrm{ob}}^{\mathrm{D}}(t) \to D_{\mathrm{r}}^{\mathrm{D}} \le D_{\mathrm{ob}}^{\mathrm{S}}$ for oblique sources, while $D_{\mathrm{t}xy(\mathrm{a}x)}^{\mathrm{D}}(t) \to \min\left(D_{\mathrm{r}}^{\mathrm{D}}, D_{\mathrm{t}xy(\mathrm{a}x)}^{\mathrm{S}}\right)$ for axial and tangential sources, where the modified decay rates of specular fields are given by

$$D_{\mathrm{ob(t}xy,\mathrm{a}x)}^{\mathrm{S}} = 10 \lg e \cdot c\, \beta_{\mathrm{Eob(t}xy,\mathrm{a}x)} / l_{\mathrm{ob}(xy,x)} \tag{27}$$

Accordingly, the decay of the total diffuse field is $D_{\mathrm{r}}^{\mathrm{D}}$ at maximum.

3.6. Integrated reverberation in rooms

Adding the energy density of specular and diffuse fields in Eqs. (13) and (24), the overall energy density in the room is expressed by

$$\begin{aligned} E(t) = \frac{4W}{c} \Bigg[& \frac{\gamma_{\mathrm{r}}}{A_{\mathrm{r}}} e^{-\frac{\alpha_{\mathrm{Er}}}{l_{\mathrm{r}}} ct} + \frac{\gamma_{\mathrm{ob}}\left(1-\mu_{\mathrm{ob}}\right)}{B_{\mathrm{ob}}} e^{-\frac{\beta_{\mathrm{Eob}}}{l_{\mathrm{ob}}} ct} \\ & + \sum_{xy} \frac{\gamma_{\mathrm{t}xy} \pi c L_x L_y}{2\omega V} \frac{2-\mu_{\mathrm{t}xy}}{\hat{B}_{\mathrm{t}xy}} e^{-\frac{\beta_{\mathrm{Et}xy}}{l_{\mathrm{t}xy}} ct} \\ & + \sum_{x} \frac{\pi c^2 L_x}{2\omega^2 V} \frac{4-\mu_{\mathrm{a}x}}{\hat{B}_{\mathrm{a}x}} e^{-\frac{\beta_{\mathrm{Ea}x}}{l_{\mathrm{a}x}} ct} \Bigg] \end{aligned} \tag{28}$$

where

$$\gamma_{\mathrm{r}} = \gamma_{\mathrm{ob}} \mu_{\mathrm{ob}} + \sum_{xy} \frac{\gamma_{\mathrm{t}xy} \pi c L_x L_y \mu_{\mathrm{t}xy}}{2\omega V} + \sum_{x} \frac{\pi c^2 L_x \mu_{\mathrm{a}x}}{2\omega^2 V},$$

Consequently, the reverberation of the total field in a rectangular room is apparently composed of eight kinds of exponential decay, which correspond to seven rates for specular fields and one for the 3D diffuse field.

4. Case study based on the new theory of reverberation

4.1. Conditions of rooms

As a case study based on the above theory, the energy density levels relative to $L_0 = 10\lg(W/c)$ are calculated for rectangular rooms with a volume 1000 m^3, an absorption area 210 m^2, and different aspect ratios and distributions of absorption (Table I), additionally assuming that the absorption and scattering coefficients have no dependence of incidence angle, and the latter has an uniform value for all surfaces. Based on the conventional diffuse field theories, the reverberation times by Sabine's equation are 0.77 sec for all cases, and those by Eyring's are 0.62 sec for Cases 1a/b, and 0.65 sec for Cases 2a/b.

Table I. Conditions of rectangular rooms.

Case	L_x (m)	L_y (m)	L_z (m)	α_x	α_y	α_z
1a	10	10	10	0.35	0.35	0.35
1b	10	10	10	0.10	0.35	0.60
2a	20	10	5	0.30	0.30	0.30
2b	20	10	5	0.10	0.20	0.40

4.2. Reverberation of non-diffuse field

As a calculated example, Figure 5 shows the energy decay of specular, diffuse and total fields for Case 1b with a scattering coefficient of 0.1, at 500 and 2000 Hz. It is seen that the decay curve of the specular field for every source group is straight, but not for the diffuse field. Compared between the two frequencies, the energy density levels of axial and tangential sources are higher, and the curvature of the total decay is more remarkable at the lower frequency.

4.3. Effect of surface scattering

Figure 6 shows the energy decay for Cases 1a/b and 2a/b, with uniformly changing the scattering coefficient from 0.05 to 0.8. In Case 1a (cube, uniform absorption), surface scattering does not affect the total decay, but remarkably does in the other cases. It is seen that with increasing the scattering coefficient, the decay of specular field steadily becomes greater, and additionally its curvature is suppressed. However, the change of scattering coefficient from 0.4 to 0.8 hardly affects the total decay in all cases.

5. Conclusions

A general theory of reverberation in rectangular rooms was developed, which is based on the image source method with decomposing 1D, 2D and 3D specular fields, and considering diffuse fields caused by surface scattering. It describes that the total reverberation is apparently composed of seven kinds of exponential decay for specular fields and one for the 3D diffuse field. A case study demonstrated the energy decay of each specular and diffuse fields, and the effect of surface scattering on the reverberation in non-diffuse fields.

Acknowledgement

This project has been funded by the Grant-in-Aid Scientific Research from Japan Society for the Promotion of Science (No. 21360275).

References

[1] W. C. Sabine: Collected paper on acoustics, Harvard Univ. Press, 1922.

[2] C. F. Eyring: Reverberation time in “dead” rooms, J. Acoust. Soc. Am. 1 (1930) 217-241.

[3] R. F. Norris: A derivation of the reverberation formula, Architectural Acoustics ed. V. O. Knudsen, Appendix II, John Wiley & Sons, New York, 1932.

[4] G. Millington: A modified formula for reverberation, J. Acoust. Soc. Am. 4 (1932) 69-82.

[5] W. J. Sette: A new reverberation time formula, J. Acoust. Soc. Am. 4 (1933) 193-210.

[6] H. Kuttruff: Weglängverteilung und Nachhallverlauf in Räumen mit diffuse reflektierenden Wänden, Acustica 23 (1970) 238-239.

[7] H. Kuttruff: Nachhall und effektive Absorption in Räumen mit diffuser Wandreflexion, Acustica 35, (1976) 141-153.

[8] D. Fitzroy: Reverberation formula which seems to be more accurate with nonuniform distribution of absorption, J. Acoust. Soc. Am. 31 (1959) 893-897.

[9] J. Pujolle: Nouvelle formule pour la durée de réverbération, Rev. d’Acoust. 19 (1975) 107-113.

[10] Y. Hirata: Geometrical acoustics for rectangular rooms, Acustica 43 (1979), 247-252.

[11] H. Arau-Puchades: An improved reverberation formula, Acustica 65 (1988) 163-179.

[12] E. Nilsson: Decay processes in rooms with non-diffuse sound fields, Report TVBA-1004, Lund Inst. Tech., 1992.

[13] R. O. Neubauer: Estimation of reverberation time in rectangular rooms with non-uniformly distributed absorption using a modified Fitzroy equation, Build. Acoust. 8 (2001) 115-137.

[14] P. M. Morse and R. H. Bolt: Sound waves in rooms, Rev. Mod. Phys. 16 (1944).

[15] M. Vorländer and E. Mommertz: Definition and measurement of random-incidence scattering coefficients, Appl. Acoust. 60 (2000) 187-200.

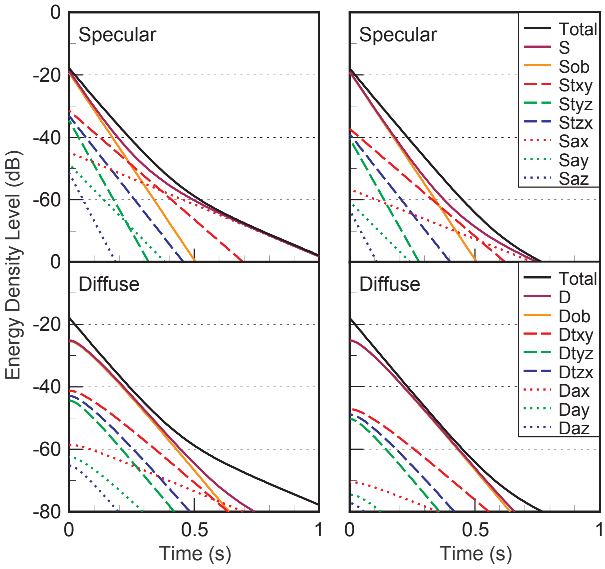

(a) 500 Hz (b) 2000 Hz

Figure 5. Energy decay of specular, diffuse and total fields for Case 1b with a scattering coefficient of 0.1: (a) 500 Hz, (b) 2000 Hz.

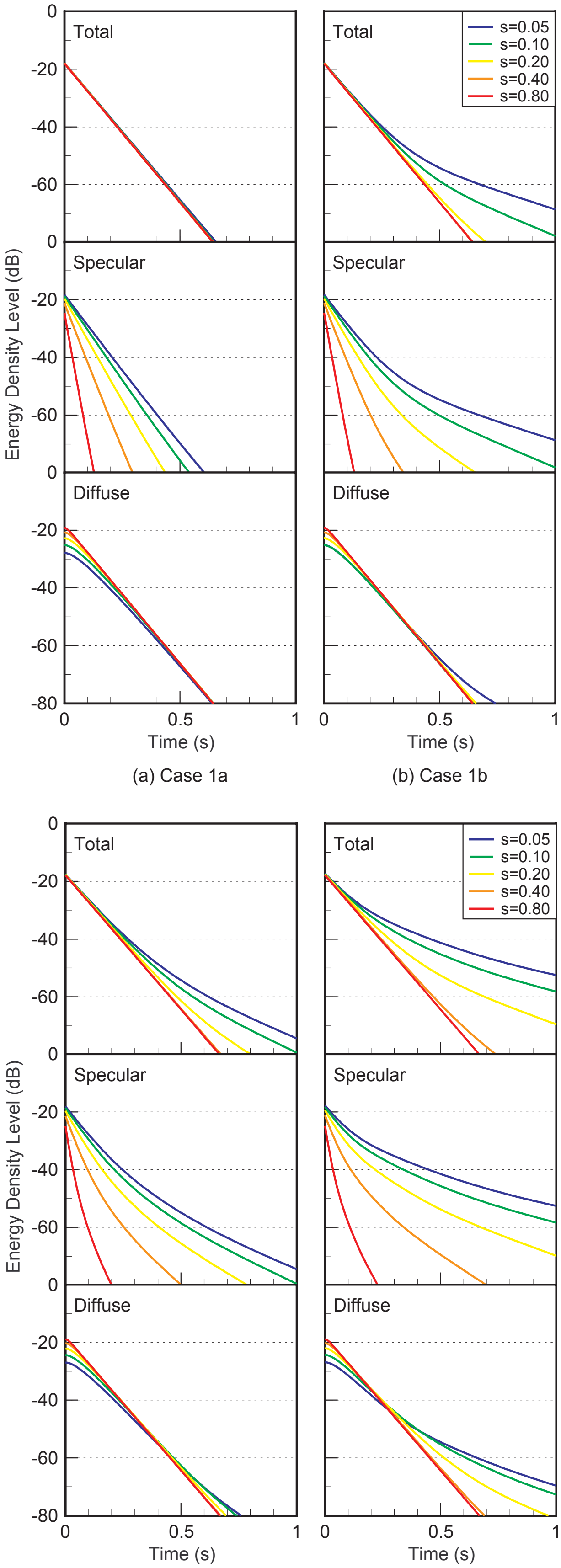

(a) Case 1a (b) Case 1b

(c) Case 2a (d) Case 2b

Figure 6. Energy decay of specular, diffuse and total fields at 500 Hz, with changing the scattering coefficient from 0.05 to 0.8: (a) Case 1a, (b) Case 1b, (c) Case 2a, (d) Case 2b.

(c) European Acoustics Association, ISBN: 978-84-694-1520-7, ISSN: 221-3767